

Hybrid Viscoelastic Modeling with Adaptive Finite Difference Staggered Grid

Fan Jiang* and Shengwen Jin, Halliburton/Landmark, Houston, TX, USA

Summary

In marine environments, high moisture content in sediments has characteristics of both a solid and liquid. It possesses a shear resistance that is independent of the rate of deformation. This scenario can be described by viscoelasticity. Viscoelastic media is used to describe hydrocarbon reservoir features, such as fluid saturation, aligned fractures, etc. This inelastic behavior is simulated by seismic viscoelastic modeling and could further improve the image quality of complex geological structures. However, conventional viscoelastic modeling requires a large computing cost with large memory requirements. In this abstract, a three-dimensional (3D) hybrid viscoelastic modeling method with an adaptive finite difference staggered grid is proposed to improve the viscoelastic modeling computing efficiency, especially in marine environments.

Introduction

Shear- and mode-converted waves provide detailed information for further improving the image quality of complex geological structures and quantification of reservoir characterization. In real earth media, the mechanical wave is dispersed and attenuated. This inelastic behavior is described by the viscoelastic model. Carcione (1993) investigated attenuation in viscoelastic media and proposed the viscoelastic wave equations. Those equations transform the time convolutions involved in the viscoelastic constitutive relationships to the first-order partial differential equations by introducing memory variables.

However, conventional viscoelastic modeling requires a huge computing cost and encounters oversampling issues (Hayashi et al. 2001). To overcome spatial oversampling with high velocity, Pitarka (1999) proposed a finite difference method for discrete, spatial differential operators in 3D elastic media. Jiang and Jin (2013) developed a hybrid acoustic-elastic modeling method using an adaptive finite difference grid in a marine environment, resulting in a tremendous improvement in computing efficiency.

In this abstract, Jiang and Jin's method (2013) is extended to perform 3D hybrid acoustic-viscoelastic modeling with an adaptive staggered grid by finite difference scheme. It combines the first-order pressure-velocity acoustic wave equation in the water layer and the stress-velocity viscoelastic wave equation in solid inelastic sediments. To absorb side boundary reflection, the unsplit convolutional perfectly matched layer (UCPML) boundary condition (Martin and Komatitsch 2009) is modified to be used with

hybrid viscoelastic modeling. Numerical examples illustrate the efficiency and accuracy of hybrid viscoelastic modeling compared to conventional fixed-grid implementation.

Method

Carcione (1993) investigated attenuation in viscoelastic media and developed the corresponding stress-velocity wave equations, where memory variables are introduced to model the relaxation mechanism. The attenuation effect is represented by quality factor Q_p (for P-wave) and Q_s (for S-wave). The relation between Q_p , Q_s , and the relaxation time in standard linear viscoelastic equations is described as below:

$$\tau_\sigma = \frac{1}{\omega} \left(\sqrt{1 + \frac{1}{Q_p^2}} - \frac{1}{Q_p} \right) \quad (1a)$$

$$\tau_\varepsilon^p = \frac{1}{\omega^2 \tau_\sigma} \quad (1b)$$

$$\tau_\varepsilon^s = \frac{1 + \omega \tau_\sigma Q_s}{\omega Q_s - \omega^2 \tau_\sigma} \quad (1c)$$

Here, τ_σ and τ_ε are the relaxation times for the P- and S-wave, respectively, and ω is frequency. Equation 1 describes a group of relaxation times for a single relaxation mechanism in a generalized standard linear solid. The related stress-strain relation with a single relaxation mechanism is described as the following:

$$\begin{aligned} \dot{\sigma}_{ij} = & \frac{\partial v_k}{\partial x_k} [\lambda(1 + \tau_\varepsilon^p) + 2\mu(1 + \tau_\varepsilon^s)] \\ & + \frac{\partial v_i}{\partial x_j} [2\mu(1 + \tau_\varepsilon^s)] + r_{ij} \quad \text{if } (i = j) \end{aligned} \quad (2a)$$

$$\dot{\sigma}_{ij} = \left(\frac{\partial v_i}{\partial x_j} + \frac{\partial v_j}{\partial x_i} \right) \mu(1 + \tau_\varepsilon^s) + r_{ij} \quad \text{if } (i \neq j) \quad (2b)$$

where σ_{ij} denotes the ij th component of the stress tensor ($i, j = 1, 2, 3$), v_i denotes the components of the particle velocities, x_i describes the spatial direction (x, y, z), r_{ij} indicates the first mechanism of memory variables, ρ is density, and f_i denotes the body force. The parameters λ and μ are used to define the P-wave and S-wave velocity at a certain frequency. In the acoustic wave equation, the pressure component is used to substitute three stress components, and no quality factor is used.

To implement hybrid viscoelastic modeling, the velocity model is split into an acoustic and viscoelastic zone (Figure

Hybrid Viscoelastic Modeling with Adaptive Finite Difference Staggered Grid

1). The first-order acoustic wave equation is applied in the water layer, and the viscoelastic wave equation is applied in inelastic sediments. The water velocity is used to calculate grid spacing in the acoustic zone, while minimum S-wave velocity is used to calculate grid spacing in the inelastic zone. Wave propagation in each zone will be implemented by different wave equations with relative grid spacing. Source energy is quickly propagated through the water layer to the sea bottom, which saves significant computational time with less memory usage.

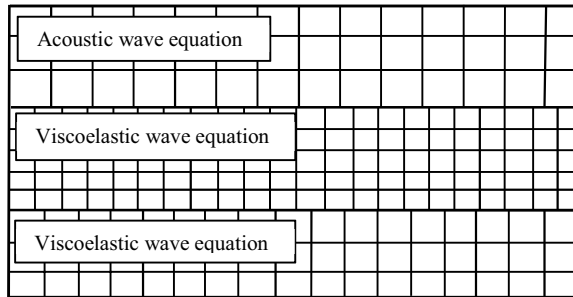


Figure 1: Grid layout of hybrid viscoelastic modeling method.

Between the upper zone and the lower zone, an overlapping zone is designed for wavefield exchange. Grid spacing in this overlapping zone varies based on velocity distribution. Variable finite difference coefficients are calculated, depending on the staggered grid position of stress and particle velocity components (Pitarke 1999). Wavefield exchange requires linear interpolation, which communicates the wavefield between the pressure component, stress components, particle velocity components, and memory variables. Variable finite difference coefficients should be created before the time step calculation to reduce computation time.

Conventional PML performs well to absorb the body wave and surface waves (Collino and Tsogka 2001) but is less efficient for the grazing incidence waves. Martin and Komatitsch (2009) developed an UCPML boundary condition to efficiently absorb the grazing incidence in the viscoelastic wave equation. In this paper, their method is extended to incorporate it with hybrid viscoelastic modeling. Because UCPML does not require splitting equations into a separate equation, this reconfiguration is straightforward. The derivative $\partial v / \partial x'$ in Equation 2 is replaced by a recursive convolutional equation with an additional array ξ :

$$\xi^{n+1} = b_x * \xi^n + a_x * \frac{\partial v}{\partial x'} \quad (3a)$$

$$\frac{\partial v^{pml}}{\partial x'} = \frac{1}{k_x} \frac{\partial v}{\partial x'} + \xi^{n+1} \quad (3b)$$

Here, v is the pressure component, stress components, or particle velocity components and a_x , b_x , and k_x are predefined damping factors in x direction. They are determined by P-wave velocity, grid spacing, and the thickness of the PML layer. x' is variable grid spacing in different velocity zones. Special treatment of UCPML in the overlapping zone is required. To absorb the same reflection energy across all zones and avoid artifacts from the overlapping zone, the thickness of the UCPML zone in each velocity zone should be identical, such as, in x direction, the thickness of UCPML zone = $\text{PML_pad1} * dx_1 = \text{PML_pad2} * dx_2 = \dots$. The same treatment should be applied to y and z directions, respectively.

Examples

A three-layer velocity model with a marine streamer acquisition geometry is tested. The model size is $NX=NY=NZ=3$ km. The water bottom is at 1-km depth. A pressure source is activated at sea surface by a Ricker wavelet with a maximum frequency of 30 Hz. The model parameters and quality factors are listed in Table 1. The same quality factor is used in all viscoelastic layers for numerical comparison.

Table1: Model parameters

| | Vp (km/s) | Vs (km/s) | Density | Qp | Qs |
|-----------------------|-----------|-----------|---------|----------|----------|
| 1 st layer | 1.6 | 0.0 | 1.0 | ∞ | ∞ |
| 2 nd layer | 2.5 | 1.3 | 2.0 | 60 | 60 |
| 3 rd layer | 3.5 | 2.5 | 3.0 | 60 | 60 |

The seismic wave in viscoelastic media distorts the energy and phase distribution of the incident and reflected wave. Figure 2a shows the acquisition geometry of a hybrid viscoelastic model. The seismic source is placed at the center of the model with five receiver cables. Figure 2b displays a snapshot from hybrid viscoelastic modeling. Different grid spacings are used in different zones. Figure 2c compares the common shot gather between hybrid elastic modeling (Jiang and Jin 2013) and the hybrid viscoelastic modeling proposed in this abstract. The phase is stretched because of the attenuation effect, and energy is diminished. Figure 2d shows a single trace comparison between elastic modeling, conventional fixed-grid viscoelastic modeling (Carcione 1993), and hybrid viscoelastic modeling. The result is well matched with the conventional result. Compared to conventional fixed-grid implementation, hybrid viscoelastic modeling saves 70% computation time, and the memory requirement is approximately 50% less than for the conventional approach.

Hybrid Viscoelastic Modeling with Adaptive Finite Difference Staggered Grid

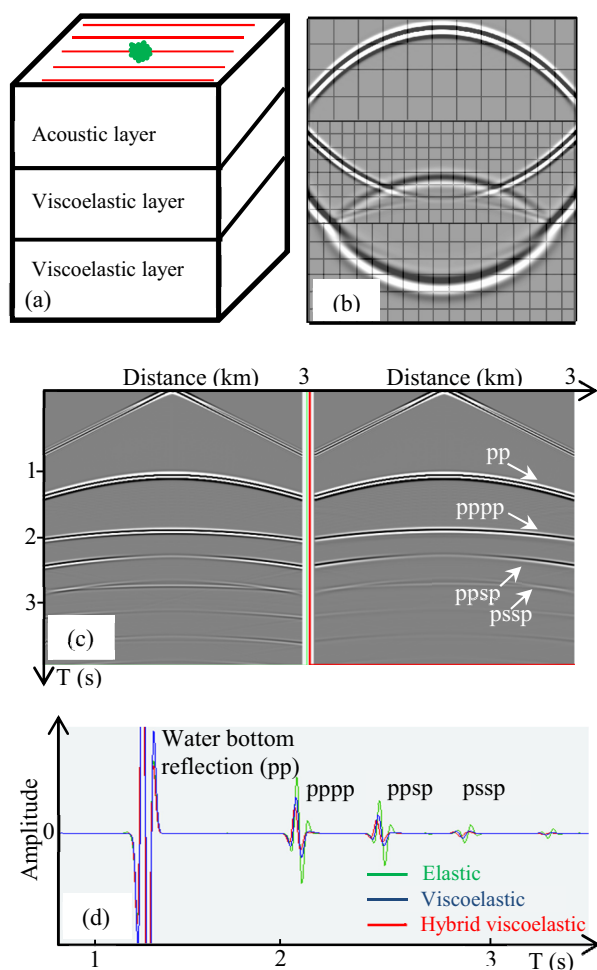


Figure 2: (a) Velocity model with acquisition geometry; (b) wavefield snapshot with different grid spacing; (c) comparison of vertical component between hybrid elastic modeling and hybrid viscoelastic modeling. Wave energy is decreased significantly with an increase in propagation time; (d) comparison of three single traces (offset = 2.6 km) generated from elastic modeling (green line), conventional fixed-grid viscoelastic modeling (blue line) (Carcione 1993), and hybrid viscoelastic modeling (red line).

Figure 3a shows amplitude spectrum analysis on six shot gathers ($Q = \infty, 100, 80, 60, 40, 20$) with first arrival and first-order water bottom reflection (WBF). Because the water layer has no attenuation and WBF contains strong energy, the result shows a similar amplitude spectrum across all frequencies. However, after muting first arrival and WBF, Figure 3b shows the amplitude variation is strongly affected by quality factor and frequency (Jin et al. 2013). This analysis indicates that strong first arrival and

WBF can affect the inelastic interpretation of a subsurface structure with improper analysis of marine data processing. Muting those strong events during the data processing step should help to obtain accurate images.

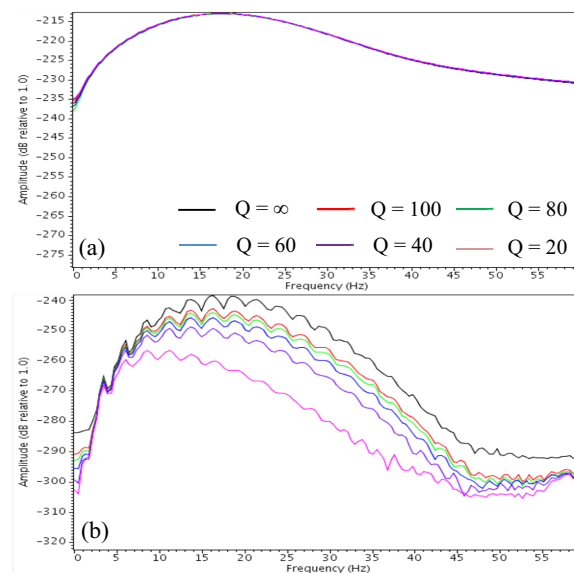


Figure 3: Amplitude spectrum analysis (a) with first arrival and first-order WBF and (b) without first arrival and first-order WBF.

A reality test was performed on the modified SEG advanced modeling (SEAM) dataset. The crossline aperture was 20 km with a depth of 15 km. A pressure source with a maximum frequency of 30 Hz was used. Figure 4a shows the P-wave velocity model. The S-wave velocity is considered as half of the P-wave velocity and is zero in the water layer. The quality factor Q_p is derived from the P-wave velocity by $Q_p = 0.04 \cdot V_p$. The quality factor in the water layer could be omitted (or assigned any value for numerical calculation) because only the acoustic wave equation is used in the water layer. In this case, sediments below the water bottom have strong attenuation ($Q_p \approx 60$), and the salt body has a relatively weak attenuation ($Q_p \approx 170$). In this test, the Q_p range is from 50 to 180. The quality factor Q_s is set to $0.8 \cdot Q_p$ empirically. As shown in Figure 4a, the velocity model is split into eight subzones, including a water zone. The minimum S-wave velocity in each subzone and maximum frequency determine grid spacing for numerical modeling. The amplitude of the converted wave in viscoelastic media decreases significantly, and high frequency energy is attenuated (Figures 4b and 4c). In this test, hybrid viscoelastic modeling uses 40% less computational time, and the memory requirement is 30% less than for the conventional fixed-grid approach. This hybrid scheme can easily extend

Hybrid Viscoelastic Modeling with Adaptive Finite Difference Staggered Grid

to vertical transverse isotropy (VTI), horizontal transverse isotropy (HTI), or orthorhombic media. For tilted transverse isotropy (TTI) media, a rotated staggered grid is required.

Conclusion

A 3D hybrid viscoelastic modeling method is proposed that combines the acoustic and viscoelastic wave equations with an adaptive finite difference staggered grid. The first-order acoustic wave equation is applied to the water layer, while the viscoelastic wave equation is applied to solid inelastic sediments. Several tests demonstrated that the new method provides results that are as accurate as with conventional fixed-grid implementation but with tremendously improved computational efficiency and a much smaller memory requirement.

Acknowledgement

The authors thank SEG for the SEAM model and Halliburton for permission to publish this paper.

References

- Carcione, J.M., 1993, Seismic modeling in viscoelastic media: *Geophysics*, **58**, 110–120.
- Collino, F. and C. Tsogka, 2001, Application of the perfectly matched absorbing layer model to the linear elastodynamic problem in anisotropic heterogeneous media: *Geophysics*, **66**, 294–307.
- Hayashi, K., D.R. Burns, and M.N. Toksoz, 2001, Discontinuous-grid finite difference seismic modeling including surface topography: *Bull. Seism. Soc. Am.*, **91**, 1750–1764.
- Jiang, F. and S. Jin, 2013, Hybrid acoustic-elastic modeling method using adaptive grid finite difference scheme in marine environment: *75th EAGE Conference & Exhibition*, Extended Abstracts, Tu 01 11.
- Jin, S., F. Jiang, and X. Zhu, 2013, Viscoelastic modeling with simultaneous microseismic sources: *83rd SEG Annual Meeting*, Expanded Abstract, 3355–3359.
- Martin, R. and D. Komatitsch, 2009, An unsplit convolutional perfectly matched layer technique improved at grazing incidence for the viscoelastic wave equation: *Geophys. J. Int.*, **179**, 333–344.
- Pitarka, A., 1999, 3-D elastic finite-difference modeling of seismic motion using staggered grids with nonuniform spacing: *Bull. Seism. Soc. Am.*, **89**, 54–68.

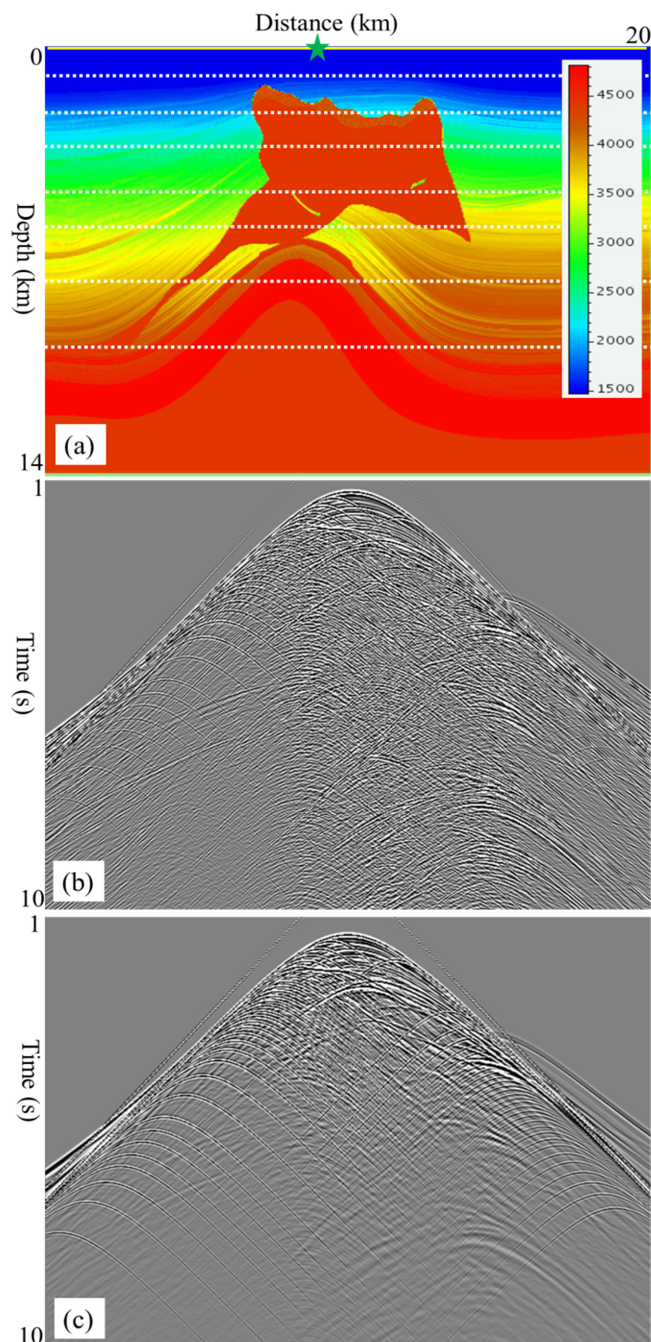


Figure 4: Viscoelastic modeling of the SEAM model: (a) P-wave velocity with eight subzones; (b) elastic gather; (c) viscoelastic gather. The green star is the source position, the yellow line is the receiver cable, and the seven dash lines indicate the subzone boundaries of the velocity model for implementation of hybrid viscoelastic modeling.